Journal of Organometallic Chemistry, 366 (1989) 377–389
Elsevier Sequoia S.A., Lausanne – Printed in The Netherlands
JOM 09676

2-Pyridonate (OPy) rhodium complexes. Crystal structure of $[\{Rh(\mu\text{-}OPy)(CO)_2\}_2]$; a chain-forming complex with alternate short and long metal–metal distances

Miguel A. Ciriano, B. Eva Villarroya, Luis A. Oro

Departamento de Química Inorgánica, Instituto de Ciencia de Materiales de Aragón, Universidad de Zaragoza-C.S.I.C. 50009 Zaragoza (Spain)

M. Carmen Apreda, Concepción Foces-Foces and Felix H. Cano

Departamento de Rayos-X, Instituto Rocasolano, C.S.I.C. Serrano 119, 28006 Madrid (Spain)

(Received November 14th, 1988)

Abstract

A facile synthesis of the complexes $[\{Rh(\mu\text{-}OPy)(diolefin)\}_2]$ (OPy = 2-pyridonate, diolefin = 1,5-cyclooctadiene (cod), 2,5-norbornadiene (nbd), tetrafluorobenzobarrelene (tfb)) is described. The complexes react with carbon monoxide to give either $[\{Rh(\mu\text{-}OPy)(CO)_2\}_2]$(V) or $[Rh_4(CO)_{12}]$ depending on the reaction conditions. Complex V reacts with triphenylphosphine to give $[Rh_2(\mu\text{-}OPy)_2(CO)_3(PPh_3)]$ and with cod to give $[(cod)Rh(\mu\text{-}OPy)_2Rh(CO)_2]$. Addition of methyl iodide to V gives the 2-acetoxypyridinerhodium(I) complex *cis*-$[RhI(2\text{-}MeCOOPy)(CO)_2]$. A single crystal X-ray structure determination has been carried out on compound V. It crystallizes in the *Pbca* space group with lattice constants *a* 19.4397(33), *b* 13.6340(16), and *c* 12.2121(12) Å. The final agreement factors were $R = 0.073$ and $R_w = 0.063$ for 2030 observed reflections. The structure of V consists of binuclear units having bridging 2-pyridonate ligands in a head-to-head disposition, which arrange in a columnar fashion forming an infinite chain with Rh(1)–Rh(2) and Rh(1)–Rh(2)$(x, \frac{1}{2} - y, \frac{1}{2} + z)$ distances of 2.899(2) and 3.410(2) Å and angles of 150.88(4) and 174.57(6)° at Rh(1) and Rh(2) respectively.

Introduction

Ligands containing angular N–C–X (X = N, O or S) bridging units are convenient building groups for the construction of multinuclear rhodium complexes containing rhodium centres in close proximity. Some representative examples of rectangular, linear or angular arrangements of the metal atoms with some of these ligands are: $[Rh_4(\mu\text{-}az)_2(\mu\text{-}Cl)_2(\mu\text{-}CO)_2(nbd)_2]$, (az = 7-azaindolate, nbd = 2,5-norborna-

0022-328X/89/$03.50 © 1989 Elsevier Sequoia S.A.

diene) [1], $[Rh_4(\mu\text{-}OPy)_2(\mu\text{-}CO)_2(CO)_4]$ (OPy = 2-pyridonate) [2], $[Rh_2(Onapy)_2(CO)_4]$ [3a], $[Rh_3(\mu\text{-}Onapy)_2(cod)_2(CO)_4]ClO_4$ [3b] (Onapy = 1,8-naphthyridine-2-one, cod = 1,5-cyclooctadiene), $[Ir_4(\mu\text{-}C_7H_4NS_2)_4I_2(CO)_8]$ ($C_7H_4NS_2$ = benzothiazole-2-thiolate) [4], and $[Rh_3(\mu\text{-}SPy)_2(CO)_6]ClO_4$ (SPy = pyridine-2-thiolate) [5]. Although there has been much interest in binuclear rhodium(II) [6a] and platinum(III) [6b] complexes containing substituted 2-pyridonate ligands bridging the two d^7 metal centres, related rhodium(I) [7a] and iridium(I) [7b] complexes have been only briefly examined. In addition there is an increasing interest in binuclear rhodium and iridium complexes having the weakly interacting d^8–d^8 electronic configuration, because they could be versatile photoreagents for the activation of otherwise inert substrates [8].

We describe here a high-yield synthesis, the crystal structure, and some reactions of the complex $[\{Rh(\mu\text{-}OPy)(CO)_2\}_2]$.

Results and discussion

The complexes $[\{M(\mu\text{-}Cl)(cod)\}_2]$ (M = Rh, Ir), were found to react readily with the anion 2-pyridonate (OPy), present in a mixture of potassium hydroxide and pyridine-2(1*H*)-one in methanol, to give the compounds $[\{M(\mu\text{-}OPy)(cod)\}_2]$ (M = Rh (**I**), Ir (**II**)) as orange or red suspensions. The related complexes $[\{Rh(\mu\text{-}OPy)(diolefin)\}_2]_x$ (diolefin = nbd (**III**), or tfb (**IV**)) are obtained in a similar way starting from the appropriate chlorodiolefinrhodium complex. An alternative route to complexes **I** and **II** involves the protonation of the methoxy group in the complexes

Table 1

Colour and analytical data for the new complexes

Compound	Colour	Yield (%)	Analysis (Found (calcd.) (%)) C	H	N	Mol. weight [a] (Found (calcd.)) in $CHCl_3$
$[\{Rh(\mu\text{-}OPy)(cod)\}_2]$	Orange	90	50.90	5.30	4.60	602
(**I**)			(51.16)	(5.28)	(4.59)	(610)
$[\{Ir(\mu\text{-}OPy)(cod)\}_2]$	Red	85	39.20	4.07	3.46	806
(**II**)			(39.58)	(4.09)	(3.55)	(789)
$[\{Rh(\mu\text{-}OPy)(nbd)\}_2]$	Red	60	50.01	4.35	4.78	565
(**III**)			(49.85)	(4.18)	(4.84)	(578)
$[\{Rh(\mu\text{-}OPy)(tfb)\}_2]$	Orange	70	47.84	2.34	3.30	842
(**IV**)			(48.25)	(2.38)	(3.30)	(845)
$[\{Rh(\mu\text{-}OPy)(CO)_2\}_2]$	Copper	70	33.30	1.60	5.70	505
(**V**)			(33.23)	(1.59)	(5.53)	(506)
$[Rh_2(\mu\text{-}OPy)_2(CO)_3(PPh_3)]$	Orange	60	50.86	3.34	3.88	756
(**VI**)			(50.29)	(3.13)	(3.78)	(740)
$[\{Rh(\mu\text{-}OPy)(CO)(PPh_3)\}_2]$	Orange	75	58.93	3.94	2.80	[a]
(**VII**)			(58.61)	(3.96)	(2.89)	
$[(cod)Rh(\mu\text{-}OPy)_2Rh(CO)_2]$	Red	60	42.96	3.56	5.18	550
(**VIII**)			(43.03)	(3.61)	(5.01)	(558)
$[RhI(CO)_2(MeCOOPy)]$	Yellow	60	25.87	1.59	3.32	420
(**IX**)			(25.55)	(1.67)	(3.31)	(423)

[a] Decomposes slowly in solution.

$[\{M(\mu\text{-MeO})(cod)\}_2]$ with pyridine-2(1H)-one ($pK_a = 11.62$) [9] in dichloromethane. Complexes I and II have been prepared recently using sodium hydride as deprotonating agent [7].

Complexes I–IV are binuclear in solution, i.e. $x = 1$, (see Table 1), and have been characterized by a combination of elemental analyses, IR and NMR spectroscopy.

Carbon monoxide reacts with the complexes $[\{M(\mu\text{-OPy})(cod)\}_2]$ at atmospheric pressure to give the tetracarbonyl compounds $[\{M(\mu\text{-OPy})(CO)_2\}_2]$ (M = Rh (V), Ir (V′)) in high yield. We recently described the preparation of complex V in lower yield by reaction of $[\{Rh(\mu\text{-Cl})(CO)_2\}_2]$ with 1-H-pyridine-2-one and potassium hydroxide in methanol under an atmosphere of carbon monoxide; in the absence of carbon monoxide the unexpected tetranuclear compound $[Rh_4(\mu\text{-OPy})_4(\mu\text{-CO})_2(CO)_4]$ is isolated.

The iridium complex V′ is air-sensitive and was not isolated analytically pure, but it shows the same pattern of ν(CO) bands (at 2070s, 2040m, 1995s, 1985sh, cm^{-1}) as the analogous rhodium complex V in solution. The latter gives unexpected ^1H and $^{13}C\{^1H\}$ NMR spectra. In addition, it displays broad ν(CO) bands in the solid state and crystallizes as dichroic dark-blue powder or long needles having a copper-like aspect, suggesting molecular stacking in the solid state. In order to

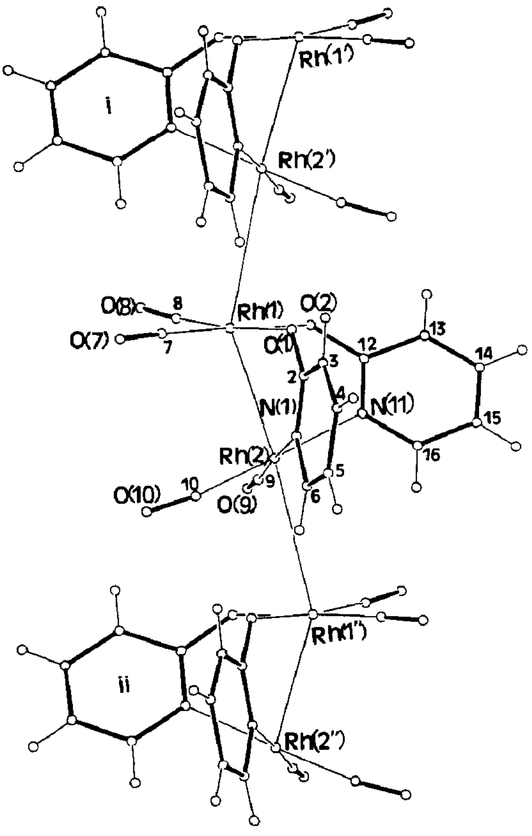

Fig. 1. ORTEP [28] view of the structure and the crystal packing of $[\{Rh_2(\mu\text{-OPy})(CO)_2\}_2]$ with the atom numbering scheme. The symbols of the carbon atoms are omitted for clarity.

Table 2

Selected geometrical parameters (i and ii refer to the symmetry operations: $x, \frac{1}{2} - y, \frac{1}{2} + z$ and $x, \frac{1}{2} - y, -\frac{1}{2} + z$, respectively)

(a) Interatomic distances (Å) and angles (°)

Rh1–Rh2(i)	3.410(2)	Rh1–Rh2	2.899(2)
Rh1–O1	2.084(9)	Rh1–O2	2.078(10)
Rh1–C7	1.819(14)	Rh1–C8	1.848(18)
C7–O7	1.155(18)	C8–O8	1.127(23)
Rh2–N1	2.088(11)	Rh2–N11	2.120(11)
Rh2–C10	1.863(16)	Rh2–C9	1.914(15)
C10–O10	1.122(20)	C9–O9	1.087(19)
N1–C2	1.367(17)	N11–C12	1.368(17)
C2–C3	1.480(22)	C12–C13	1.399(22)
C3–C4	1.373(24)	C13–C14	1.330(25)
C4–C5	1.356(23)	C14–C15	1.361(26)
C5–C6	1.397(22)	C15–C16	1.344(20)
C6–N1	1.345(17)	C16–N11	1.348(18)

Rh1–Rh2–Rh1(ii)	174.57(6)	Rh2–Rh1–Rh2(i)	150.88(4)
C7–Rh1–C8	90.7(7)	C10–Rh2–C9	90.7(6)
C7–Rh1–O1	89.5(5)	C10–Rh2–N1	90.7(6)
C7–Rh1–O2	177.7(6)	C10–Rh2–N11	177.0(6)
O1–Rh1–O2	88.8(4)	N1–Rh2–N11	88.1(4)
O1–Rh1–C8	175.0(6)	N1–Rh2–C9	178.2(5)
O2–Rh1–C8	91.1(6)	N11–Rh2–C9	90.5(5)
O7–C7–Rh1	176.1(13)	O10–C10–Rh2	174.9(14)
O8–C8–Rh1	175.7(17)	O9–C9–Rh2	176.0(13)
Rh1–O1–C2	128.4(9)	Rh1–O2–C12	126.5(9)
Rh2–N1–C2	119.9(9)	Rh2–N11–C12	122.3(9)
Rh2–N1–C6	120.8(9)	Rh2–N11–C16	118.8(9)
O1–C2–N1	122.1(12)	O2–C12–N11	119.4(13)
O1–C2–C3	119.5(13)	O2–C12–C13	123.9(13)
C2–N1–C6	119.2(11)	C12–N11–C16	118.9(12)
N1–C2–C3	118.4(13)	N11–C12–C13	116.7(12)
C2–C3–C4	118.7(15)	C12–C13–C14	122.9(16)
C3–C4–C5	121.5(16)	C13–C14–C15	119.4(16)
C4–C5–C6	117.9(14)	C14–C15–C16	118.2(15)
C5–C6–N1	124.2(13)	C15–C16–N11	123.8(14)

(b) Some torsion angles (°)

Rh1–Rh2–N11–C12	−22.0(10)	Rh1–Rh2–N1–C2	−21.0(9)
Rh2–N11–C12–O2	4.0(7)	Rh2–N1–C2–O1	6.8(17)
N11–C12–O2–Rh1	31.5(18)	N1–C2–O1–Rh1	25.0(18)
C12–O2–Rh1–Rh2	−36.9(11)	C2–O1–Rh1–Rh2	−31.1(10)
O2–Rh1–Rh2–N11	22.6(4)	O1–Rh1–Rh2–N1	20.3(4)
C7–Rh1–Rh2–C10	23.1(7)		
C8–Rh1–Rh2–C9	20.6(7)		

(c) Dihedral angles (°). (Deviations (Å) of rhodium atoms in brackets)

1: O1,O2,C7,C8	[Rh1: 0.031(1)	Rh2: 2.772(1)]
2: N1,N11,C9,C10	[Rh2: 0.015(1)	Rh1: −2.834(1)]
3: N1,C2,C3,C4,C5,C6	[Rh1: −0.775(1)	Rh2: 0.175(1)]
4: N11,C12,C13,C14,C15,C16	[Rh1: −0.891(1)	Rh2: 0.147(1)]

Planes	Angles (°)	Planes	Angles (°)
1–2	29.5(4)	2–3	63.7(4)
1–3	86.6(5)	2–4	76.5(5)
1–4	59.9(5)	3–4	80.9(5)

Table 3

Final atomic coordinates

Atom	x	y	z
Rh1	0.15070(5)	0.19290(7)	0.11350(9)
Rh2	0.15422(5)	0.25498(7)	−0.11346(8)
O1	0.2353(5)	0.2866(7)	0.1085(8)
N1	0.2563(5)	0.2888(8)	−0.0763(8)
C2	0.2756(7)	0.3025(9)	0.0302(12)
C3	0.3472(9)	0.3334(11)	0.0529(13)
C4	0.3905(8)	0.3506(13)	−0.0338(14)
C5	0.3705(9)	0.3336(14)	−0.1385(12)
C6	0.3027(7)	0.3034(12)	−0.1564(12)
C7	0.2085(7)	0.0882(11)	0.1072(13)
O7	0.2478(6)	0.0250(8)	0.0996(11)
C8	0.0761(10)	0.1104(13)	0.1312(15)
O8	0.0329(7)	0.0570(11)	0.01466(13)
O2	0.0870(5)	0.3153(7)	0.1161(10)
N11	0.1255(6)	0.3897(8)	−0.0399(9)
C12	0.0951(7)	0.3941(11)	0.0610(9)
C13	0.0728(8)	0.4865(12)	0.0961(15)
C14	0.0833(8)	0.5680(12)	0.0386(17)
C15	0.1144(9)	0.5621(10)	−0.0610(14)
C16	0.1346(8)	0.4734(10)	−0.0968(12)
C9	0.0601(8)	0.2282(10)	−0.1486(10)
O9	0.0062(6)	0.2114(11)	−0.1626(11)
C10	0.1809(8)	0.1342(12)	−0.1709(12)
O10	0.1964(7)	0.0588(9)	−0.1980(10)

ascertain the structure of complex V and the arrangement in the crystal an X-ray diffraction study was undertaken.

Figure 1 illustrates the coordination geometry and the atomic numbering scheme. The main geometrical characteristics and the final atomic parameters for the non-hydrogen atoms are given in Tables 2 and 3, respectively. The complex is binuclear. Each rhodium atom is bonded to two terminal carbonyl groups in *cis* positions and to two bridging 2-pyridonate ligands to complete a square-planar coordination around each metal centre. The coordination planes are slightly twisted, making a dihedral angle of 29.5(4)°.

One of the striking features of the structure is the coordination of the bridging ligands through the oxygen atoms to one of the rhodium atoms and through the nitrogen atoms to the other. In other words, the bridging ligands are arranged in a head-to-head fashion in such a way that the chemical environments of the two rhodium atoms are different.

Another striking feature of the structure is the arrangement of the binuclear units in a columnar fashion to form an infinite zig-zag chain with Rh(1)–Rh(2) and Rh(1)–Rh(2)($x, \frac{1}{2} - y, \frac{1}{2} + z$) distances of 2.899(2) and 3.410(2) Å and angles of 150.88(4) and 174.57(6)° at Rh(1) and Rh(2), respectively. The average minimum pseudotorsion angle about the Rh(1)–Rh(2) vector is 21.7(2)° (see Table 2b).

The Rh–C, Rh–N and Rh–O coordination distances are within the usual range, as in the related complex $[Rh_4(\mu\text{-}OPy)_4(\mu\text{-}CO)_2(CO)_4]$ [2]. In the 2-pyridonate ligands, the C(2)–C(3) and C(12)–C(13) bond distances are the longest which was noted previously [10] even in the free pyridine-2(1*H*)-one, which is like the keto tautomer, but they are shorter in the 6-chloropyridine-2-ol, which is like the enol tautomer [11]. In addition, the C(2)–O(1) and C(12)–O(2) distances (1.26(2) and 1.28(2) Å) are intermediate between those of a single (1.43 Å) [12a] and a double (1.20 Å) [12b] C–O bond. This is indicative of an extensive π-electron delocalization in the N–C–O moiety.

In the present complex the C(2)–N(1)–C(6) and C(12)–N(11)–C(16) angles are smaller. 119.2(11) and, 118.9(12)°, respectively, than those, 123.5(3)°, in the pyridine-2(1*H*)-one. Similarly the O(1)–C(2)–C(3) and O(2)–C(120–C(13) adjacent angles are 119.5(13) and 123.9(13)°, compared with 125.9(3)° in the pyridine-2(1*H*)-one. The rings are planar.

The ^{1}H NMR spectra of complex V in solution at variable temperature, shown in Fig. 2, are not consistent with the structure found in the solid state. The rigid head-to-head isomer (HH), having C_s symmetry, should display four resonances for the equivalent 2-pyridonate bridges. Instead, two sets of four resonances of the same intensity are observed at low and room temperature. Before the crystal structure was determined, we thought that these results might be due to a lack of symmetry in the molecule, but that is now evidently not the case. In addition, the ^{13}C{^{1}H} NMR spectrum of V also shows twice the number of resonances than expected, e.g. four doublets for the carbonyl groups, pointing to the presence of a 1/1 mixture of the head-to-head (HH) and head-to-tail (HT) isomers (shown in Fig. 3) in solution. Interconversion of these isomers occurs rapidly at 50°C, giving rise to averaged signals in the ^{1}H NMR spectrum. Interestingly, this interconversion must lead to the crystallization of the HH isomer from solutions of complex V, probably due to an additional stabilization arising from the extended metal–metal interaction. In contrast, the related compound [{Rh(μ-SPy)(CO)$_2$}$_2$] is present as the HT isomer both in the solid state and in solution [13]. In this context, SCF calculations carried out on model isomers of the type [Rh$_2$(SCHNH)$_4$] indicate that the HT isomer equivalent is about 10 kcal more stable than the HH isomer, if it is assumed that only electronic factors control the equatorial coordination [14]. However, the coordination in axial positions in d^7–d^7 complexes and possible steric effects of the bridging ligands may complicate matters [6b].

Complex V reacts with carbon monoxide in dichloromethane/hexane under pressure (4 bar) to give yellow solutions of the cluster $Rh_4(CO)_{12}$, whereas brown crystals of $Rh_6(CO)_{16}$ are obtained if the reaction is carried out in methanol, parelleling the reduction of [{Rh(μ-OMe)(cod)}$_2$] by carbon monoxide [15].

Triphenylphosphine carries out stepwise replacement of the carbonyl groups in complex V, readily giving the compound [Rh$_2$(μ-OPy)$_2$(CO)$_3$(PPh$_3$)] (VI) (ν(CO): 2070s, 1995s, 1975vs cm^{-1} in CH$_2$Cl$_2$). Replacement of a second carbonyl group takes place under more forcing conditions to give [{Rh(μ-OPy)(CO)(PPh$_3$)}$_2$] (VII) (ν(CO) 1965s cm^{-1} in CH$_2$Cl$_2$). The reaction is readily reversed when carbon monoxide is bubbled through a solution of complex VII. In fact, complex VII loses triphenylphosphine in solution, as was shown by measuring its molecular weight, and so the equilibrium 1 must lie far over to the left.

$$[Rh_2(\mu\text{-OPy})_2(CO)_3(PPh_3)] \underset{+CO}{\overset{+PPh_3}{\rightleftharpoons}} [\{Rh(\mu\text{-OPy})(CO)(PPh_3)\}_2] \qquad (1)$$

The triphenylphosphine ligands are expected to replace the carbonyl groups *trans* to nitrogen atoms (which have a stronger *trans* effect than oxygen atoms), as

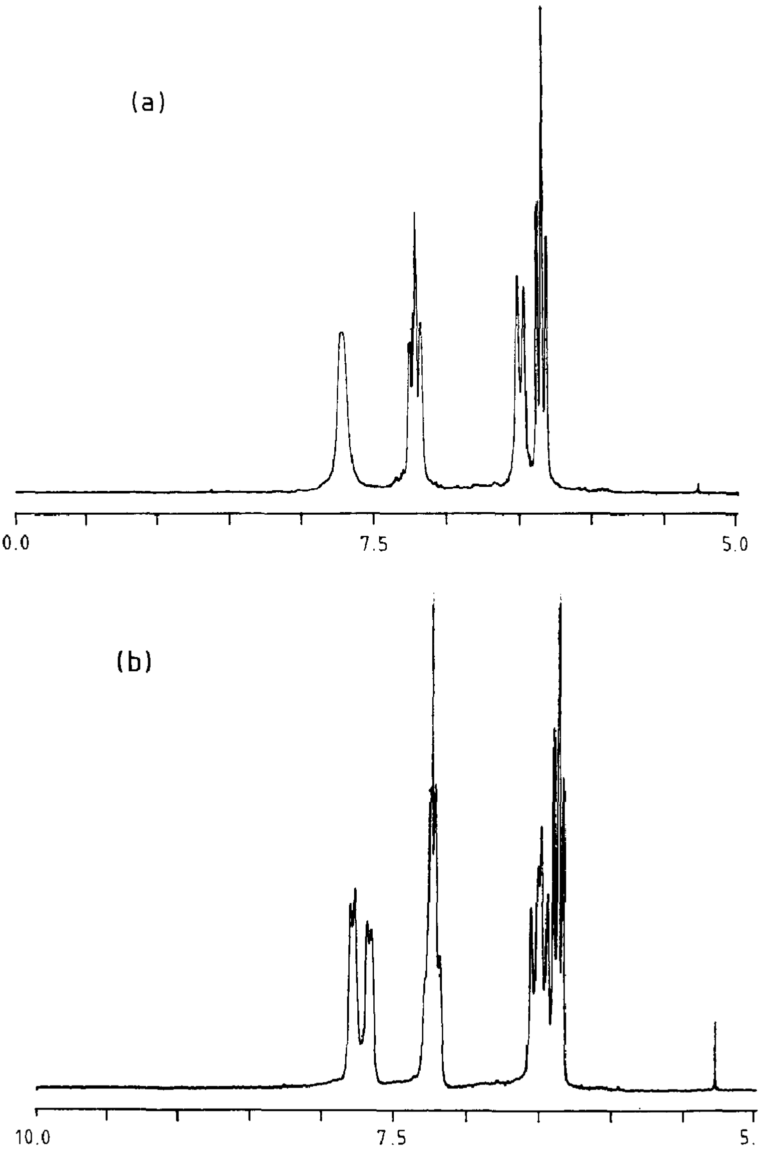

Fig. 2. ^{1}H NMR spectra of complex V at 50 ° C (a), at 20 ° C (b).

observed for the mononuclear complexes [Rh(oxinate)(CO)$_2$] [16] and [Rh(O$_2$CPy)-(CO)$_2$] [17]. Complexes VI and VII show identical ^{31}P{^{1}H} NMR spectra, displaying one doublet resonance (at δ 44.5 ppm, ^1J(RhP) 160 Hz) in accordance with the proposed structures (see Fig. 4).

Stepwise replacement of the carbonyl groups in complex V by 1,5-cyclooctadiene in hexane can be also carried out. Monitoring of the reaction by IR spectroscopy reveals that the complex [(cod)Rh(μ-OPy)$_2$(CO)$_2$] (VIII) is formed and it can be isolated in good yield as red-green dichroic crystals. If left, the reaction goes further, to give eventually complex II.

Complex VIII is binuclear in solution and shows two ν(CO) bands (at 2065s, 2000s cm^{-1} in hexane) characteristic of the *cis*-dicarbonylrhodium moiety, while

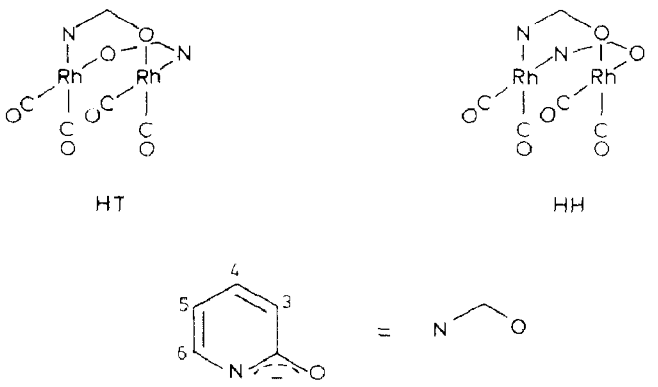

Fig. 3. HH and HT isomers of complex V.

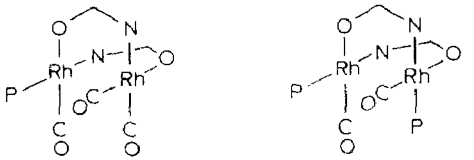

Fig. 4. Proposed structures for complexes VI and VII.

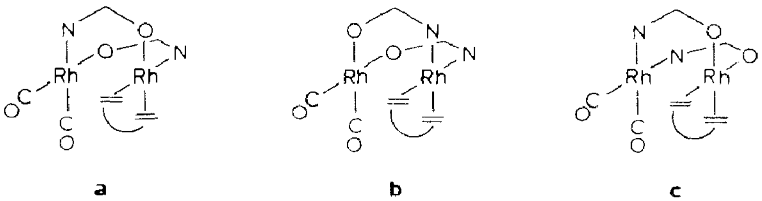

Fig. 5. Isomers of complex VIII.

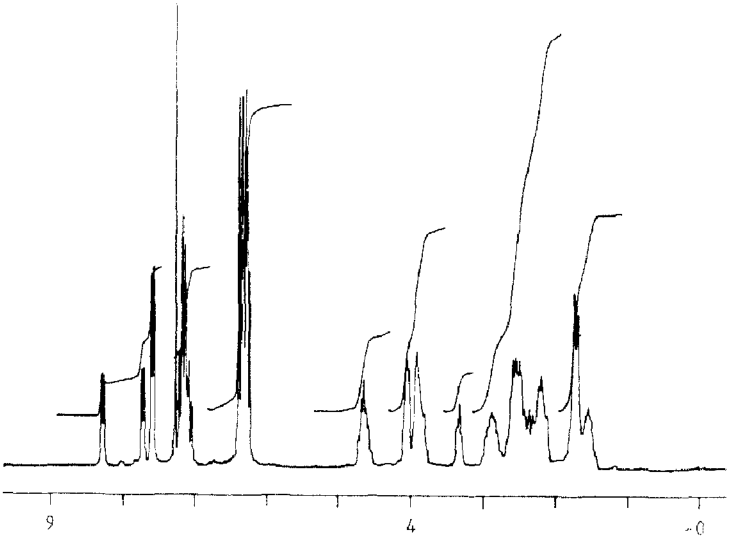

Fig. 6. ^{1}H NMR of complex VIII at −50 ° C.

VIII in a Nujol mull displays three broad ν(CO) bands in the 2100–1950 cm^{-2} region. The dichroism and the broadening of the ν(CO) bands in the solid state again suggest the presence of extended molecular interactions in complex VIII, as in the case of complex V. Like V, complex VIII exists in solution as an equimolecular mixture of two isomers of structures, (a) and either (b) or (c) (Fig. 5), as indicated by the ^{1}H NMR spectrum (Fig. 6). The most deshielded protons (H6) in the 2-pyridonate ligands give rise to two doublets for the isomer (a) and one doublet for either isomer (b) or (c). Noteworthy is the absence of one of the head-to-head isomers, probably (c), even though interconversion of the structures in solution occurs rapidly at slightly above room temperature.

Complex V undergoes an oxidative-addition with iodine to give an insoluble dark-brown solid showing ν(CO) bands due to terminal and bridging carbonyl groups (at 2050s and 1860s cm^{-1} in Nujol). Its insolubility precludes further characterization. Methyl iodide reacts with complex V to give a mixture of slightly soluble compounds showing ν(CO) bands nearly at 2025 s and 1840s cm^{-1}. However, if the reaction is carried out under an atmosphere of carbon monoxide a yellow solid analyzing as the mononuclear complex [Rh(Me)I(OPy)(CO)$_3$] is obtained. This compound was identified by IR, ^{13}C{^{1}H}, and ^{1}H NMR spectroscopy as, surprisingly, the rhodium(I) complex [RhI(MeCOOPy)(CO)$_2$] (IX), containing the 2-acetoxypyridonate ligand as follows. Complex IX shows two ν(CO) bands at 2080 s and 2010 s cm^{-1} due to a *cis*-dicarbonylrhodium moiety. An additional ν(CO) band at 1785 cm^{-1} could perhaps be assigned to an acetyl group, but its frequency is high compared to that for the acetyl complexes [{Rh(μ(SPy)I(COMe)(CO)}$_2$] (1710 cm^{-1}) [18]. This and another band near 1200 cm^{-1} agree well with those found for organic esters. In addition, a deshielded singlet resonance for a methyl group not bonded to rhodium is observed in the ^{13}C{^{1}H} and ^{1}H NMR spectra of complex VIII. Moreover, the lack of coupling with the rhodium nucleus and the chemical shift of the resonance at δ 169 ppm in the ^{13}C{^{1}H} NMR spectrum are in accordance with the presence of a MeCOOR group, and rule out the acetyl possibility. Furthermore, complex VIII can also be isolated from the bridge splitting reaction of [{Rh(μ-I)(CO)$_2$}$_2$] with 2-acetoxypyridine, although in solution

$$[\{Rh(\mu\text{-}I)(CO)_2\}_2] + 2MeCOOPy \rightleftharpoons 2[RhI(CO)_2(MeCOOPy)] \qquad (2)$$

there is equilibrium 2. Because of this, ν(CO) bands of both carbonyl compounds are observed both in the reaction mixture and in solutions of complex IX.

The generation of the 2-acetoxypyridine ligand from complex V and methyl iodide implies an initial oxidative-addition reaction, such as occurs in absence of carbon monoxide. The fate of the binuclear unit is unknown. It can either break up into a mononuclear complex, as happens in the oxidative-addition of chlorine to [{Ir(μ-POy)(cod)$_2$)}$_2$] [7a], or undergo insertion of carbon monoxide into the Rh–Me bond to give an acetyl complex. (Formation of the diacetyl complex [{Rh(μ-SPy)(COMe)(CO)}$_2$] occurs in the reaction of the related complex [{Rh(μ-SPy)(CO)$_2$}$_2$] with methyl iodide [13].) Possible alternatives are shown in Scheme 1.

In the case of the mononuclear complex the carbonyl group can insert into either the Rh–Me or the Rh–O bonds. The first is a well-known process and is the more probable. The second would be the inverse of the decarbonylation of 8-quinolylformate catalyzed by [RhCl(PPh$_3$)$_3$] [18]. A reductive-elimination reaction eventu-

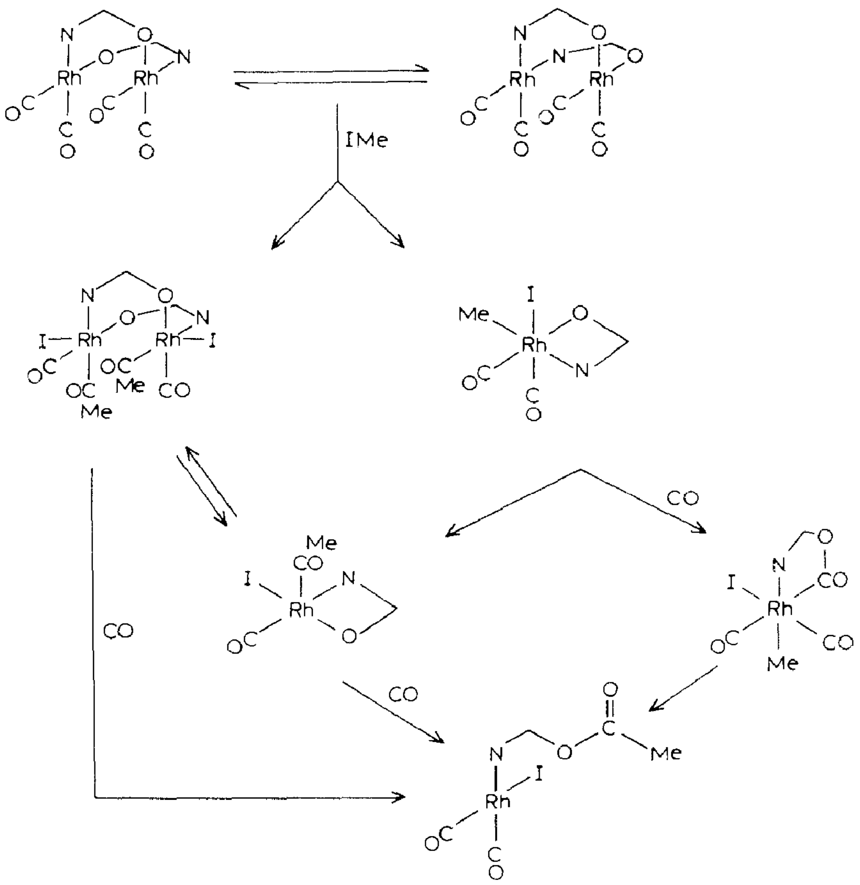

Scheme 1

ally results in formation of the MeCOOPy unit, which remains coordinated to the metal centre through the nitrogen atom.

Experimental

General comments

The complexes [{Rh(μ-Cl)(diolefin)}$_2$] (diolefin = cod [19], nbd [20] or tfb [21]), [{Ir(μ-C)(cod)}$_2$] [22], [{M(μ-OMe)(cod)}$_2$] (M = Rh or Ir) [23] were prepared by published methods. Elemental analyses were carried out with a Perkin-Elmer 240B microanalyzer. IR spectra (range 4000–200 cm^{-1}) were recorded on a Perkin-Elmer 597 spectrophotometer using Nujol mulls between polyethylene sheets or dichloromethane solutions. ^{1}H, ^{13}C{^{1}H} and ^{31}P{^{1}H} NMR spectra were recorded with a Varian XL-200 spectrometer operating at 200.57, 50.309 and 80.984 MHz, respectively. Reactions were carried out at room temperature under oxygen-free nitrogen. Solvents were purified by standard methods. Analytical data for the compounds are listed in Table 1.

Preparation of complexes

[{M(μ-OPy)(cod)}$_2$] (M = Rh(I) or Ir(II)). Solid [{M(μ-Cl)(cod)}$_2$] (0.01 mmol) was treated with a solution of pyridin-2(1*H*)-one (19 mg, 0.2 mmol) and potassium

hydroxide in methanol (2 ml, 0.02 mmol) for 15 min. The mixture was concentrated to ca. 2 ml and water (1 ml) was added to complete precipitation of complex I. The solids were filtered off, washed with methanol/water (1/1) (complex I) or cold methanol (complex II), and vacuum-dried.

[{Rh(μ-Opy)(diolefin)}₂] (diolefin = nbd (III) or tfb (IV)). Solid [{Rh(μ-Cl)(diolefin)}$_2$] (0.1 mmol) was added to a mixture of pyridin-2(1*H*)-one (19 mg, 0.2 mmol) and potassium hydroxide in methanol (2 ml, 0.2 mmol) to give orange or red solutions of complexes III and IV. The solvent was pumped off, the residue extracted with dichloromethane and the extract filtered. Concentration of the filtrate to ca. 1 ml and slow addition of cold hexane gave the complex III and IV as microcrystalline solids which were filtered off, washed with cold hexane, and vacuum-dried.

[{Rh(μ-Opy)(CO)$_2$}$_2$] (V). Dry carbon monoxide was bubbled through a dichloromethane solution (10 ml) of complex I (91.5 mg, 0.15 mmol) for 15 min to give a dark red solution. Hexane (10 ml) was then added and the bubbling was continued for 2 h, to give dichroic deep-blue or copper-like crystals, which are filtered off, washed with cold hexane, and vacuum-dried. ^{13}C{^{1}H} NMR of the isomers (CDCl$_3$, 20 °C) δ (ppm): 185.2 (d, ^1J(Rh–C) 67 Hz, CO), 184.3 (d, ^1J(Rh–C) 71.5 Hz, CO), 183.9 (d, ^1J(Rh–C) 68 Hz, CO), 183.3 (d, ^1J(Rh–C) 71.4 Hz, CO), 171.9 (2C, C2 and C2′, OPy), 148.0, 147.5, 135.5 (2C), 117.8, 117.4, 112.0, 111.8 (8C, C3, C3′, C4, C4′, C5, C5′, C6, C6′, OPy). (The primed numbers correspond to the second isomer).

[{Rh$_2$(μ-Opy)$_2$(CO)$_3$(PPh$_3$)}] (VI). A solution of PPh$_3$ (39.3 mg, 0.15 mmol) in dichloromethane (3 ml) was added dropwise to one of complex V (76 mg, 0.15 mmol) in the same solvent (3 ml). The resulting orange solution was stirred for 15 min and then concentrated to ca. 1 ml. Addition of hexane gave a precipitate of complex VI, which was filtered off, washed with hexane, and vacuum-dried.

[{Rh(μ-Opy)(CO)(PPh$_3$)}$_2$] (VII). Solid V (50.6 mg, 0.1 mmol) was added to a solution of PPh$_3$ (52.4 mg, 0.2 mmol) in diethyl ether (10 ml). The mixture was stirred for ca. 30 min until an orange solid was formed. Hexane was then added to complete the precipitation. The solid was filtered off, washed with hexane/diethyl ether (2/1), and vacuum-dried.

[(cod)Rh$_2$(μ-OPy)$_2$(CO)$_2$] (VIII). Solid V (76 mg, 0.15 mmol) was added to a solution of 1,5-cyclooctadiene (18.4 ml, 0.15 mmol) in hexane (10 ml) and the mixture refluxed for 2 h. The resulting orange solution was concentrated to ca. 2 ml and cooled at −10 °C to give red crystals, which were filtered off, washed with cold hexane, and vacuum-dried. ^{1}H NMR of the mixture isomers (CDCl$_3$, −50 °C) δ (ppm): 8.28 (d, 1H, H6, OPy, isomer HT), 7.72 (d, 1H, H6′, OPy, isomer HT), 7.59 (d, 2H, H6, OPy, isomer HH), 7.2–7.0 (overlapping m., 4H, OPy), 6.4–6.2 (overlapping m., 4H, OPy), 4.8 (m, 2H, HC=C{cod}), 4.1 (m, 2H, HC=C{cod}), 3.9 (m, 3H, HC=C{cod}), 3.25 (m, 1H, HC=C{cod}), 2.9 (m, 2H, CH$_2${cod}), 2.8–2.1 (overlapping m., 8H, CH$_2${cod}), 1.8–1.4 (overlapping m., 6H, CH$_2${cod}).

[RhI(CO)$_2$(MeCOOpy)] (IX). Methyl iodide (0.30 ml, 4.8 mmol) was added to a solution of complex V (50.6 mg, 9.1 mmol) in dichloromethane/hexane (2/3) (10 ml), and the mixture was kept for 6 h under an atmosphere of carbon monoxide at room temperature. The resulting yellow solution was concentrated under an atmosphere of carbon monoxide to give yellow crystals of IX. The solvent was removed by syringe, and the solid was washed with cold hexane then dried under a stream of

carbon monoxide. ^{1}H NMR ($CDCl_2$, 20 °C), δ (ppm): 8.63 (d, 1H, H6); 8.03 (t of d, 1H, H4); 7.44 (t, 1H, H5); 7.35 (d, 1H, H3); 2.5 (s, 3H, CH_3). $^{13}C\{^1H\}$ NMR ($CDCl_2$, 20 °C), δ (ppm): 181.4 (broad d, ^1J(Rh–C) 69 Hz), 167.2 (O–C=O); 157.4 (C2); 150.7, 141.5, 122.6, 118.9 (C3, C4, C5, C6); 21.5 (CH_3).

Table 4

Crystal data and data collection parameters

Crystal data	
Formula	$C_{14}H_8N_2Rh_2O_6$
Crystal habit	Prismatic, rectangular base
Crystal size (mm)	0.23 × 0.12 × 0.02
Symmetry	Orthorhombic, *Pbca*
Unit cell determination	Least-squares fit from 72 reflections ($\theta < 45°$)
Unit cell dimensions (Å)	19.4397(33), 13.6340(16), 12.2121(12)
Packing: V (Å^3), Z	3236.7(7), 8
Dc (g cm^{-3}), M, $F(000)$	2.077, 506.04, 1952
μ (cm^{-1})	172.1
Experimental data:	
Technique	Four circle diffractometer Bisecting geometry Graphite oriented monochromator: Cu-K_α $\omega/2\theta$ scan, scan width: 1.50° Detector apertures 1 × 1°, 1 min/refl.
Total measurements	Up to 65°
Number of reflections:	
measured	2743
independent	2743
observed	2030 ($3\sigma(I)$ criterion)
Standard reflections	2 reflections every 90 minutes Variation: no
Max-min transmission factors:	1.241–0.578 [DIFABS]
R values before and after absorption correction:	0.153–0.100
Solution and refinement:	
Solution	Patterson function and DIRDIF System
Refinement	L.S. on F_{obs} with 1 block
Parameters:	
number of variables	217 (H parameters were kept fixed)
degrees of freedom	1813
ratio of freedom	9.4
H atoms	Difference synthesis
Final average shift/error	0.05
Weighting-scheme	Functions: $w = K/[f^2(F_{obs})] \cdot [g(\sin\theta/\lambda)]$ K = scale factor to ensure $\langle \omega\Delta^2 F \rangle \sim 1$
Max. thermal value	U_{33}(08) = 0.13(1) Å^2
Final ΔF peak	1.13 e Å^{-3} near Rh atoms
Final R and R_w	0.073–0.063
Computer and programs	VAX 11/750, DIFABS [24], X-RAY65 System [25], DIRDIF [26]
Scattering factors	Int. Tables for X-ray Crystallography [27]

X-Ray data collection

Crystal data and details of data collection are given in Table 4.

Acknowledgements

We thank Prof. F. Bonati (Universita di Camerino) and Dr. S. Castillon (Universidad de Barcelona en Tarragona) for valuable discussions, and CAICYT for financial support.

References

1 L.A. Oro, M.A. Ciriano, B.E. Villarroya, A. Tiripicchio and F.J. Lahoz, J. Chem. Soc., Chem. Commun., (1984) 521; (1985) 1891.

2 M.A. Ciriano, L.A. Oro, B.E. Villarroya, M.C. Apreda, C. Foces-Foces and F.H. Cano, J. Chem. Soc., Dalton Trans., (1987) 981.

3 (a) A.M. Manotti-Lanfredi, A. Tiripicchio, R. Usón, L.A. Oro, M.A. Ciriano and B.E. Villarroya, Inorg. Chim. Acta, 88 (1984) L9; (b) A. Tiripicchio, F.J. Lahoz, L.A. Oro, M.A. Ciriano and B.E. Villarroya, ibid., 111 (1986) L1. M.A. Ciriano, B.E. Villarroya and L.A. Oro, ibid., 120 (1986) 43.

4 L.A. Oro, M.A. Ciriano, F. Viguri, A. Tiripicchio, M. Tiripicchio-Camellini and F.J. Lahoz, Nouv. J. Chim., 10 (1986) 75.

5 M.A. Ciriano, S. Sebastian, L.A. Oro, A. Tiripicchio, M. Tiripicchio-Camellini and F.J. Lahoz, Angew. Chem., 100 (1988) 406; Angew. Chem. Int. Ed. Engl., 27 (1988) 402.

6 (a) F.A. Cotton, S. Han and W. Wang, Inorg. Chem., 23 (1984) 4762 and refs. therein; (b) D.P. Bancroft and F.A. Cotton, ibid., 27 (1988) 1633 and refs. therein.

7 (a) G.S. Rodman and K.R. Mann, Inorg. Chem., 24 (1985) 3507; (b) T. Sielisch and M. Cowie, Organometallics, 7 (1988) 707.

8 A. Viček Jr. and H.B. Gray, J. Am. Chem. Soc., 109 (1987) 286 and refs. therein.

9 A. Albert and J.N. Phillips, J. Chem. Soc., (1956) 1294.

10 L.S. Hollis and S.J. Lippard, J. Am. Chem. Soc., 105 (1983) 3494.

11 J. Almlof, A. Kvick and I. Olovsson, Acta Crystallogr., B, 27 (1981) 1201.

12 (a) S.G. Wilkinson in D. Barton and W.D. Ollis (Eds.), Comprehensive Organic Chemistry, Pergamon Press, Oxford, 1979, Vol. 1, p. 582; (b) R. Brettle, ibid., Vol. 1, p. 945.

13 L.A. Oro, M.A. Ciriano, F. Viguri, A. Tiripicchio, M. Tiripicchio-Camellini and F.J. Lahoz, J. Chem. Soc. Dalton Trans., in press.

14 J.M. Poblet and M. Bernard, Inorg. Chem., 27 (1988) 2935.

15 A. Vizi-Orosz, G. Pályi and L. Markó, J. Organomet. Chem., 57 (1973) 379.

16 J.G. Leipoldt, S.S. Basson and C.R. Dennis, Inorg. Chim. Acta, 50 (1981) 121.

17 J.G. Leipoldt, G.J. Lamprecht and D.E. Graham, Inorg. Chim. Acta, 101 (1985) 123.

18 J.M. Suggs and G.A.N. Pearson, Tetrahedron Lett., 21 (1980) 3853.

19 G. Giordano and R.H. Crabtree, Inorg. Synth., 19 (1979) 218.

20 E.A. Abel, M.A. Bennett and G. Wilkinson, J. Chem. Soc., (1959) 3178.

21 D.E. Roe and A.G. Massey, J. Organomet. Chem., 28 (1971) 273.

22 J.L. Herde, J.C. Lambert and C.V. Senoff, Inorg. Synth., 15 (1974) 18.

23 R. Usón, L.A. Oro and J.A. Cabeza, Inorg. Synth., 23 (1985) 126.

24 N. Walker and D. Stuart, Acta Cryst. A, 39 (1983) 158.

25 J.M. Stewart, P.A. Machin, C.W. Dickinson, H.L. Ammon, H. Heck and H. Flack, TR-446, The X-RAY System, University of Maryland, U.S.A., 1976.

26 P.T. Beurskens, W.P. Bosman, H.M. Doesburg, R.O. Gould, Th.E.M. Van den Hark, P.A.J. Prick, J.H. Noordijk, G. Beurskens, V. Parthasarathi, H.J. Bruins Slot and R.C. Haltiwanger, DIRDIF System, Crystallography Laboratory, Toernooiveld, Nijmegen, The Netherlands, 1984.

27 International Tables for X-Ray Crystallography, Vol 4, Kynoch Press, Birmingham, 1974.

28 C.K. Johnson, Report ORNL-3794, Oak Ridge National Laboratory, Oak Ridge TN, 1965.